MICROMECHANICAL COMPUTATIONAL MODELING OF RESERVOIR COMPACTION AND SURFACE SUBSIDENCE

Márcio A. Murad **João N. Guerreiro**
Abimael F.D. Loula *

Abstract

A micromechanical computational model of overburden subsidence and compaction of a naturally fractured reservoir due to fluid extraction is proposed. The deformable reservoir is characterized by two levels of hydrodynamics (flow in micro and macropores) and its computational treatment is based on a micromechanical analysis of dual porosity systems, i.e. media locally characterized by a porous matrix composed of permeable matrix blocks and the surrounding system of fractures. The homogenization technique is applied to upscale the constitutive relations available in the fine structure to the field scale. Application of this procedure yields a microstructure model of dual porosity type, wherein the poroelastic matrix blocks act as distributed sources/sinks of mass and momentum to the global macroscopic medium. The microstructural model is able to incorporate delayed secondary subsidence phenomenon, which is induced by creep effects arising from the delayed drainage of the fluid in the micropores. A two-level finite element method is proposed to solve the coupled micro-macro governing equations of dual porosity type. Numerical experiments are performed showing the influence of creep effects on the surface subsidence of an oil-field during primary recovery. The results show the strong potential of the proposed formulation in solving coupled hydro-mechanical problems with microstructure which commonly appear in reservoir simulation.

*The authors were partially supported by a research grant from FAPERJ (Cientista do Nosso Estado)
AMS Subject Classification: Primary 73xx, 76xx, Secondary 73Q05, 76S05
Key words and Phrases: Reservoir Subsidence, dual porosity, Secondary Reservoir Compaction, homogenization, two-level finite element method

Resumo

Um modelo computacional micromecânico é proposto para descrever os processos de subsidência e compactação de um reservatório naturalmente fraturado durante o processo de extração de fluido. O reservatório deformável é caracterizado por dois níveis de hidrodinâmica e seu tratamento computacional é baseado em uma análise micromecânica de meios porosos com dois niveis de porosidade, isto é o meio é caracterizado por uma matriz porosa composta por blocos permeáveis bem como o sistema de fissuras. A técnica de homogeneização é aplicada no processo de transferência de escala do modelo constitutivo da escala fina para a de campo. Aplicação deste procedimento conduz a elaboração de um modelo de porosidade dupla onde os blocos poroelásticos são tratados como termos de fonte distribuidos no modelo macroscópico. Métodos de elementos finitos em duas escalas são propostos na resolução do modelo acoplado de porosidade dupla. Experimentos numéricos são realizados os quais ilustram a influência da drenagem secundaria sobre a subsidência de um campo de óleo durante a prospecção primaria. Os resultados mostram o potencial da formulação proposta em resolver problemas relativos a microestrutura que frequentemente surgem em simulação de reservatórios.

1. Introduction

The extraction of oil or gas in reservoirs with weak formations is commonly characterized by a drop in the pore fluid pressure coupled with a gradual increase in the stress state of the rock matrix inside the reservoir. Before exploration, the weight of the sediments overlaying a producing formation is partially supported by the rock matrix and pore fluid pressure. As the reservoir pore pressure is depleted, the mechanical load is gradually transferred to the reservoir rock matrix (effective stresses) inducing significant reservoir compaction. Among other effects, one of the key issues related to this consolidation mechanism is the settlement of the surface of the reservoir, which is commonly referred to as *subsidence* of the overburden [11].

Reservoir compaction and overburden subsidence are of major concern in hydrocarbon reservoirs with weak formations. Although these phenomena are not common they can result in extreme environmental and financial problems. For example, areas near the sea level can be seriously affected by coastal flooding as a consequence of a considerable degree of reservoir compaction. In the sea exploration, surface subsidence can lower the deck of the platform below the sea level and consequently may cause structural instability problems. Surface subsidence is also often significant and costly when the increase in effective stress generate shear stresses in the overburden which may lead to well casing damage. The most severe surface subsidence occurs when the oil-field is under primary recovery, prior to implementation of waterfloods for pressure support. Even in the primary stage, the development of an efficient computational model to accurately simulate coupled reservoir compaction and pressure depletion is not an easy task. The modeling of such problems requires a coupled analysis of both hydrodynamics and geomechanical deformation in order to handle the oil-field scenario in a realistic manner.

The analysis of reservoir compaction and surface subsidence has been pursued within framework of phenomenological models developed directly at the macroscale. The reservoir matrix (poroelastic or poroplastic) is commonly treated as a single structure, i.e. a solid skeleton composed of one or more fluids saturating the wide void spaces and the impermeable deformable solid phase. On the other hand many types of porous media exhibit two hierarchical geometric structures with properties radically different from each other. For example, a fissured rock is composed by a number of porous and permeable blocks or cells separated from each other by a developed system of highly permeable fissures and thus may be characterized as a medium with a dual porosity structure. In the macroscopic picture of a dual porosity medium, the interconnected network of macropores (voids, fissures) provides most of the global permeability for macroscopic flow whereas the relatively low-permeability cells (matrix blocks) merely serve to provide storage and play the role of distributed source/sinks transfer functions of mass and momentum to the global medium. The hierarchical structure of dual porosity systems with their multiple time and space scales demand multiple scale analysis to better quantify the interaction between global and local systems [7], [8]. As this interchange at the macroscale is strongly influenced by microstructural effects, an efficient pore scale description of the double-porosity structure is crucial in order to correctly predict the overall subsidence of the surface.

To illustrate the paramount importance of micromechanical analysis on reservoir subsidence consider the so-called time-dependency aspects of the consolidation process. It is well known that reservoir consolidation usually comprises two different phenomena. The primary consolidation stage, where the reservoir deformation is mainly dictated by the coarse-grained structure (e.g. pore pressure dissipation in the macropores) and creep or secondary compaction, which is commonly referred to as the additional deformation of the skeleton associated with the delayed response of the microstructure due to hydro-mechanical perturbations of the primary stage. The secondary compaction stage is mainly dictated by *creep* effects which are characterized as an ongoing subsidence mechanism which takes place during and after the fluid pressure in the macropores has been substantially dissipated [21]. Attempts have been made to characterize creep and stress relaxation using phenomenological hereditary poroviscoelastic models wherein the stresses in the rock matrix are represented in terms of functionals of the strain history [5]. An accurate representation of time-dependent secondary creep is crucial to predict the ultimate amounts of compaction and subsidence [17]. For example, in [20] it is reported a real case where ten years after depletion of the reservoir and stop of fluid withdrawal, the subsidence rate is still ongoing due to the secondary compression stage.

One may observe that specific macroscopic features of fissured rocks, such as secondary compression and hereditary creep phenomena can explicitly be correlated with microstructure response. This correlation provides a way of representing poroviscoelastic effects in terms of the double-porosity structure of the medium. The derivation of a computational model capable of incorporating this micromechanical feature can be accomplished within the framework of microstructure models of dual porosity type (see e.g. [7], [8] for flow in rigid fissured media). This approach is based on a double covering of the porous medium by two distinct, interacting coexisting systems: the macroscopic medium, related to the macropore system (void spaces, fissures) and the microscopic one, which is represented by the permeable cells containing the micropores. The macroscopic picture associated with a microstructure model of dual porosity type is a continuous distribution of cells with prescribed geometry over the macroscopic domain, with each cell identified with a macroscopic location. The global and local systems are coupled via microstructural transfer functions which locally quantify mass and momentum interchange between them. This represents a way to recognize the geometry of the local structure and the multiple space and time scales involved in the problem.

In this paper we aim at generalizing the computational dual porosity models developed in [7] to the case where the solid matrix undergoes elastic deformations. To this end we upscale the micromechanics which consists of Biot's theory of poroelasticity [8] for the permeable cells coupled to the Stokesian fluid movement in the system of wide voids. The scale up procedure is accomplished using the homogenization technique and leads to a generalized dual porosity model for deformable fractured media wherein a global system of stress-flow governing equations appears coupled (in both hydro and mechanical sense) to a family of local consolidation problems within each cell. Variational formulation and the corresponding two-level finite element approximations are proposed to discretize the dual porosity system. Two-scale computations are obtained by invoking the Galerkin procedure at both levels. Numerical simulations of a compacting oil reservoir and its subsidence at the surface are performed showing numerically the correlation between the microstructure and macroscopic hereditary creep phenomena governing delayed secondary compression.

2. Micromechanical Analysis

Consider a hierarchical elastic porous skeleton infiltrated by a two-state fluid occupying micro and macro-pores. The porous medium is characterized by three distinct scales. The microscopic scale, which is related to the size of the micropores $\mathcal{O}(10^{-3}m)$. The intermediate mesocale associated with the size of the macro-pores, of the same order of the Darcy scale of the homogenized poroelastic blocks $\mathcal{O}(10^{-1}m)$, and the macroscopic scale of the entire reservoir which is

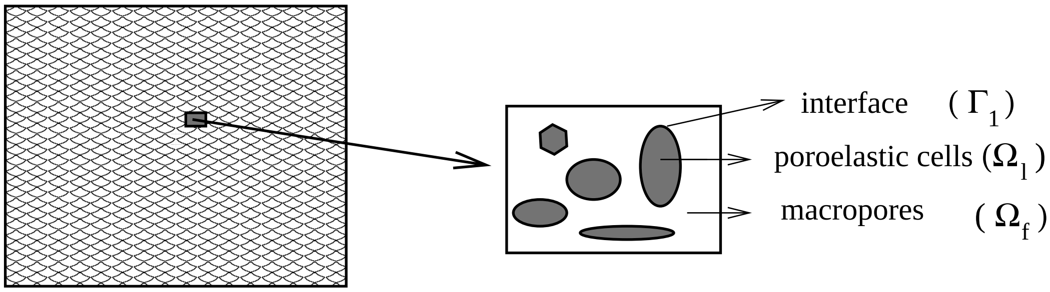

Fig 1: The microscopic geometry of a dual porosity medium

very large (usually $> \mathcal{O}(10^2 m)$. The micromechanical analysis proposed herein is related to the development of a two-scale method where we refer to as *microscale* the intermediate mesocale where the medium is composed of permeable cells (matrix blocks whose effects of the micro-pores have been already homogenized) surrounded by a system of macropores (wide void spaces, fissures). The media occupy non-overlapping domains Ω_l and Ω_f respectively and their hydromechanical interaction takes place at the common microscopic interface Γ_1 (Fig. 1). Each permeable cell is considered a Biot medium, i.e. treated as a two-phase poroelastic mixture composed of a fluid-saturated elastic solid matrix with micropores. Assume that the poroelastic cells form a disconnected system, i.e. they are isolated from each other by the macrovoids. Following the terminology of fissured media, this configuration is termed a *totally fissured medium* (TFM). A porous medium which exhibits interaction between the matrix blocks through their interfaces is termed partially fissured medium (PFM) (see [8]).

2.1. Linear Poroelastic Model for the Matrix Blocks

Consider the poroelastic matrix blocks occupying the domain Ω_l, an isothermal homogenized mixture composed of a slightly compressible fluid and an isotropic elastic homogeneous solid phase with incompressible solid grains. Assume that body forces are negligible and the solid matrix undergoes quasi-static small deformations from an initial undeformed natural state such that all higher-order nonlinear effects are neglected. The classical linearized equations of the theory of poroelasticity [6] governing cell consolidation are presented below, for each time $t \in (0, \infty)$

Overall Mass Balance

$$\overline{\phi}_l \frac{\partial \rho_l}{\partial t} + \overline{\rho}_l \Big(\mathrm{div} \boldsymbol{q}_l + \mathrm{div} \frac{\partial \boldsymbol{u}_s}{\partial t} \Big) = 0 \quad \text{in} \quad \Omega_l$$

where ρ_l is the fluid density, $\boldsymbol{u}_s$ denotes the microscopic displacement of the solid phase and $\boldsymbol{q}_l$ is the Darcy's velocity of the fluid relative to the solid phase, i.e. $\boldsymbol{q}_l \equiv \phi_l(\boldsymbol{v}_l - \partial \boldsymbol{u}_s / \partial t)$, where $\boldsymbol{v}_l$ is the fluid velocity and ϕ_l is the fluid volume fraction. The overline symbol denotes the evaluation of a property at the reference configuration. Since the medium is assumed homogeneous at the reference configuration, $\overline{\rho}_l$ and $\overline{\phi}_l$ are constants.

Total Momentum

$$\mathrm{div} \boldsymbol{t} = 0 \qquad \text{in} \quad \Omega_l \,.$$

where $\boldsymbol{t}$ is the overall microscopic stress tensor of the poroelastic cells.

Terzaghi's Decomposition

$$\boldsymbol{t} = -p_l \boldsymbol{I} + \boldsymbol{t}_s^e \qquad \text{in} \quad \Omega_l \tag{1}$$

where $\boldsymbol{I}$ is the identity tensor and p_l and $\boldsymbol{t}_s^e$ denote respectively the microscopic pore pressure and effective stress tensor.

Linear Elastic Constitutive Law

$$\boldsymbol{t}_s^e = \lambda_s \mathrm{div} \boldsymbol{u}_s \boldsymbol{I} + 2\mu_s \boldsymbol{\nabla}^s \boldsymbol{u}_s \qquad \text{in} \quad \Omega_l$$

where $\boldsymbol{\nabla}^s \boldsymbol{u}_s = 1/2(\boldsymbol{\nabla} \boldsymbol{u}_s + \boldsymbol{\nabla} \boldsymbol{u}_s^T)$ and $\{\mu_s, \lambda_s\}$ denote the pair of Lamé coefficients of the poroelastic cells.

Equation of State of the Slightly Compressible Fluid

$$p_l = \frac{1}{\overline{\rho}_l \beta_l} (\rho_l - \overline{\rho}_l) \qquad \text{in} \quad \Omega_l$$

where β_l denotes fluid compressibility.

Darcy's Law

$$\boldsymbol{q}_l = -K_l \boldsymbol{\nabla} p_l \qquad \text{in} \quad \Omega_l$$

where K_l is the hydraulic conductivity of the permeable cells.

2.2. Stokes Flow in the Macropore System

Consider the domain Ω_f occupied by a slightly compressible Stokesian fluid. Neglecting inertial, convective and gravity effects, the fluid movement in Ω_f is governed by the linearized system

$$\begin{aligned}
&\operatorname{div}\boldsymbol{t}_f = 0 \\
&\boldsymbol{t}_f = -p_f \boldsymbol{I} + \boldsymbol{\tau}_f \\
&\boldsymbol{\tau}_f = \lambda_f \operatorname{div}\boldsymbol{v}_f \boldsymbol{I} + 2\mu_f \boldsymbol{\nabla}^s \boldsymbol{v}_f \qquad \text{in} \quad \Omega_f \\
&\frac{\partial \rho_f}{\partial t} + \overline{\rho}_f \operatorname{div}\boldsymbol{v}_f = 0 \\
&p_f = \frac{1}{\overline{\rho}_f \beta_f}(\rho_f - \overline{\rho}_f)
\end{aligned} \tag{2}$$

In the above system, the subscript f is used to designate the corresponding properties in the macropore system, $\boldsymbol{v}_f$ and $\boldsymbol{\tau}_f$ denote respectively fluid velocity and viscous part of $\boldsymbol{t}_f$ and $\{\lambda_f, \mu_f\}$ denotes the pair of bulk and shear viscosities.

2.3. Boundary and Initial Conditions

The above microscopic governing equations are supplemented by initial conditions and boundary conditions on the cell-macrovoid interface Γ_1. Continuity of mass and the normal component of total stresses on Γ_1 requires

$$\begin{aligned}
&\boldsymbol{q}_l \cdot \boldsymbol{n}^1 = \boldsymbol{v}_{fs} \cdot \boldsymbol{n}^1 \\
&\boldsymbol{t}\boldsymbol{n}^1 = \boldsymbol{t}_f \boldsymbol{n}^1 \qquad \text{on} \quad \Gamma_1
\end{aligned} \tag{3}$$

where $\boldsymbol{n}^1$ is the unit normal exterior to Ω_l and $\boldsymbol{v}_{fs} \equiv \boldsymbol{v}_f - \partial \boldsymbol{u}_s / \partial t$ is the velocity of the fluid in the macropores relative to the solid phase. Moreover an additional equation is required to match fluid conditions at Γ_1. The balance of forces in the fluid phase acting in the normal direction to the interface requires

$$\boldsymbol{t}_f \boldsymbol{n}^1 \cdot \boldsymbol{n}^1 = -p_l \qquad \text{on} \quad \Gamma_1 \tag{4}$$

Finally, denoting $\boldsymbol{\tau}^1$ a unit tangent vector to the interface, following Beavers and Joseph [4] (or Saffman [18]), postulate the following "slip" boundary condition

$$\boldsymbol{\nabla}^s \boldsymbol{v}_f \boldsymbol{n}^1 \cdot \boldsymbol{\tau}^1 = \frac{\alpha}{\sqrt{k^*}} (\boldsymbol{q}_l - \boldsymbol{v}_{fs}) \cdot \boldsymbol{\tau}^1 \qquad \text{on} \quad \Gamma_1 \tag{5}$$

where $K_l = k^*/\mu_l$, with k^* and μ_l denoting respectively the permeability and viscosity of the fluid in the poroelastic cells and α is a scalar which depends on the geometry of the porous medium. The above result furnishes a compatibility condition between the shear stress and the "slip" in the tangential component of the velocity at the interface. Using (2) and (1), boundary conditions (4) and (3) can be rewritten as

$$\boldsymbol{\tau}_f \boldsymbol{n}^1 \cdot \boldsymbol{n}^1 = p_f - p_l \qquad \text{on} \quad \Gamma_1 \tag{6}$$

$$\boldsymbol{t}_s^e \boldsymbol{n}^1 \cdot \boldsymbol{n}^1 = 0 \qquad \text{on} \quad \Gamma_1$$

In particular eq. (6) shows that the jump in fluid pressure across the boundary is correlated to the shear stress $\boldsymbol{\tau}_f$ which from (2) and (5) is associated with the slip in tangential velocity. For simplicity and ease exposition in what follows we neglect the "slip" in the tangential velocity by assuming a very small slip coefficient $\alpha/\sqrt{k^*}$ in (5) and thus enforce pressure continuity $p_f = p_l \quad \text{on} \quad \Gamma_1$. Physically, the above assumption describes the physics correctly provided the interfacial resistance to tangential flow is small. Denoting l a local characteristic length, the range wherein continuity in fluid pressure across the interface can be assumed is usually quantified by large values of the Biot number $Bi_T \equiv \alpha l/\sqrt{k^*}$, which consists of the dimensionless quantity that measures the ratio between the square root of the hydrodynamical cell resistance $(1/\sqrt{k^*})$ and interfacial resistance to tangential flow $(1/\alpha l)$. When the Biot number is large, interfacial resistance to shear effects can be neglected and thus continuity in pressure can be enforced.

Finally, assuming initially an incompressible response of the poroelastic cells and that both fluids within the micro and macropores are at the same pressure $\overline{p}$, the initial conditions are

$$p_f = p_l = \overline{p}, \quad \mathrm{div}\boldsymbol{u}_s = 0 \qquad \text{in} \quad \Omega_i, t = 0, \qquad i = l, f\,.$$

3. Homogenization

The scale up procedure to the macroscale is accomplished using the homogenization procedure. In this framework our macroscopic reservoir is idealized as a bounded domain Ω^ε with a periodic structure. We then introduce microscopic and macroscopic length-scales associated with the cell (l) and with the overall dimensions of the reservoir (L). Define the ratio $\varepsilon \equiv l/L$. Consider Ω^ε composed of spatially repeated unit disjoint parallelepiped periods, Q^ε, congruent to a standard Q consisting of matrix blocks Q_l completely surrounded by a connected macropore domain Q_f. Let the systems of macropores and permeable cells in Ω^ε be denoted by Ω_f^ε and Ω_l^ε respectively. Our starting point, $\varepsilon = 1$, corresponds to the microscopic model. The ε-model in Ω^ε consists of properly scaled equations on a lattice of copies εQ. The basic problem is to investigate the asymptotics of the solution as $\varepsilon \to 0$ and therefore obtain an homogenized limit as the scale of the inhomogeneity tends to zero. The formal homogenization process [19] is accomplished by considering every property depending on both global and local length scales in the form $f = f(\boldsymbol{x}, \boldsymbol{y})$, where $\boldsymbol{x}$ and $\boldsymbol{y}$ are the macroscopic and microscopic coordinates respectively. Postulate two-scale asymptotic expansions for the set $\boldsymbol{u}^\varepsilon$ of the unknowns $\{\boldsymbol{u}_s, \boldsymbol{q}_l, \rho_l, p_l, \boldsymbol{t}, \boldsymbol{t}_s^e, \}$ and $\{\boldsymbol{t}_f, \boldsymbol{v}_f, p_f, \rho_f\}$ in terms of the perturbation parameter ε

$$\boldsymbol{u}^\varepsilon = \boldsymbol{u}^0 + \varepsilon \boldsymbol{u}^1 + \varepsilon^2 \boldsymbol{u}^2 + \ldots \tag{7}$$

with the coefficients $\boldsymbol{u}^i$, Q-periodic in $\boldsymbol{y}$. To describe the physics properly, the coefficients must be scaled. From the standard homogenization procedure of the Stokes problem, the viscosity coefficients $\{\mu_f, \lambda_f\}$ are rescaled by ε^2 [19]. In addition, to control the cell-macrovoid mass transfer within a fixed volume as $\varepsilon \to 0$, it is also necessary to scale the hydraulic conductivity of the cells K_l^ε. Following [7], this is done by the scaling law $K_l^\varepsilon = K_l \varepsilon^2$. This scaling has the effect of making the cells progressively less permeable as $\varepsilon \to 0$ and consequently prevents the degeneration of the cell-macropore mass transfer. Insert the expansions (7) into the set of microscopic governing equations with the differential operator ∂/∂_x replaced by $\partial/\partial_x + \varepsilon^{-1}\partial/\partial_y$ (recall that $\boldsymbol{y} = \varepsilon^{-1}\boldsymbol{x}$). After a formal matching of the powers of ε, we obtain a recursive system of cell problems parametrized by $\boldsymbol{x}$. For the fluid in the macropore system we have

$$\boldsymbol{t}_f^0 = -p_f^0 \boldsymbol{I} \tag{8}$$

$$\mathrm{div}_y \boldsymbol{t}_f^0 = -\boldsymbol{\nabla}_y p_f^0 = 0 \tag{9}$$

$$\mathrm{div}_x \boldsymbol{t}_f^0 + \mathrm{div}_y \boldsymbol{t}_f^1 = 0 \tag{10}$$

$$\mu_f \triangle_{yy} \boldsymbol{v}_f^0 + (\lambda_f + \mu_f) \boldsymbol{\nabla}_y \mathrm{div}_y \boldsymbol{v}_f^0 - \boldsymbol{\nabla}_y p_f^1 - \boldsymbol{\nabla}_x p_f^0 = 0 \tag{11}$$

$$\mathrm{div}_y \boldsymbol{v}_f^0 = 0 \tag{12}$$

$$\beta_f \frac{\partial p_f^0}{\partial t} + \mathrm{div}_x \boldsymbol{v}_f^0 + \mathrm{div}_y \boldsymbol{v}_f^1 = 0 \tag{13}$$

whereas for the poroelastic cells

$$\mu_s \triangle_{yy} \boldsymbol{u}_s^0 + (\lambda_s + \mu_s) \boldsymbol{\nabla}_y \mathrm{div}_y \boldsymbol{u}_s^0 = 0 \tag{14}$$

$$\mathrm{div}_y \boldsymbol{t}^0 = 0 \tag{15}$$

$$\mathrm{div}_x \boldsymbol{t}^0 + \mathrm{div}_y \boldsymbol{t}^1 = 0 \tag{16}$$

$$\boldsymbol{t}^0 = -p_l^0 \boldsymbol{I} + \boldsymbol{t}_s^{e0} \tag{17}$$

$$\boldsymbol{t}_s^{e0} = \lambda_s (\mathrm{div}_x \boldsymbol{u}_s^0 + \mathrm{div}_y \boldsymbol{u}_s^1) \boldsymbol{I} + 2\mu_s (\boldsymbol{\nabla}_x^s \boldsymbol{u}_s^0 + \boldsymbol{\nabla}_y^s \boldsymbol{u}_s^1) \tag{18}$$

$$\boldsymbol{q}_l^0 = 0 \tag{19}$$

$$\boldsymbol{q}_l^1 = -K_l \boldsymbol{\nabla}_y p_l^0 \tag{20}$$

$$\frac{1}{M} \frac{\partial p_l^0}{\partial t} + \mathrm{div}_y \boldsymbol{q}_l^1 + \mathrm{div}_x \frac{\partial \boldsymbol{u}_s^0}{\partial t} + \mathrm{div}_y \frac{\partial \boldsymbol{u}_s^1}{\partial t} = 0 \tag{21}$$

along with the boundary and initial conditions

$$\left(\boldsymbol{v}_f^0 - \frac{\partial \boldsymbol{u}_s^0}{\partial t} \right) \cdot \boldsymbol{n}^1 = 0 \tag{22}$$

$$\boldsymbol{q}_l^1 \cdot \boldsymbol{n}^1 = \left(\boldsymbol{v}_f^1 - \frac{\partial \boldsymbol{u}_s^1}{\partial t} \right) \cdot \boldsymbol{n}^1 \tag{23}$$

$$(2\mu_s \boldsymbol{\nabla}_y^s \boldsymbol{u}_s^0 + \lambda_s \mathrm{div}_y \boldsymbol{u}_s^0 \boldsymbol{I})\boldsymbol{n}^1 = 0 \qquad \text{on} \quad \Gamma_1 \tag{24}$$

$$(\boldsymbol{t}^0 - \boldsymbol{t}_f^0)\boldsymbol{n}^1 = 0 \tag{25}$$

$$(\boldsymbol{t}^1 - \boldsymbol{t}_f^1)\boldsymbol{n}^1 = 0 \tag{26}$$

$$p_l^0 = p_f^0 \tag{27}$$

$$p_l^0 = p_f^0 = \overline{p} \quad \text{and} \quad \mathrm{div}_x \boldsymbol{u}_s^0 = \mathrm{div}_y \boldsymbol{u}_s^1 = 0, \qquad \text{in} \quad \Omega_i, t = 0, \qquad i = l, f\,.$$

Next we formally collect our homogenized results.

Non-Oscillating Variables

From (9) we have $p_f^0 = p_f^0(\boldsymbol{x}, t)$. Also note that $\boldsymbol{u}_s^0$ satisfies the Neumann problem given by (14) and (24), whose solution is $\boldsymbol{u}_s^0 = \boldsymbol{u}_s^0(\boldsymbol{x}, t)$.

Macroscopic Darcy's Law

For given $p_f^0 = p_f^0(\boldsymbol{x}, t)$ and $\boldsymbol{u}_s^0 = \boldsymbol{u}_s^0(\boldsymbol{x}, t)$ combine (11),(12) with boundary condition (22) together with the assumption of a non-slip condition in the tangential direction to the interface Γ_1 to obtain a Stokes problem in terms of $\{\boldsymbol{v}_f^0, p_f^1\}$.

$$\begin{aligned} \mu_f \triangle_{yy} \boldsymbol{v}_f^0 \quad &- \quad \boldsymbol{\nabla}_y p_f^1 = \boldsymbol{\nabla}_x p_f^0 \quad \text{in} \quad \Omega_f \\ \mathrm{div}_y \boldsymbol{v}_f^0 \quad &= \quad 0 \qquad\qquad\qquad \text{in} \quad \Omega_f \\ \boldsymbol{v}_f^0 \quad &= \quad \frac{\partial \boldsymbol{u}_s^0}{\partial t} \qquad\qquad \text{on} \quad \Gamma_1 \end{aligned}$$

The homogenization of the above problem has been widely discussed in the literature [19]. Introduce the mean value operator

$$\widetilde{\cdot} = |Q|^{-1} \int_{Q_\alpha} \cdot \, dQ_\alpha, \quad \alpha = l, f$$

together with the macroscopic volume fractions of the cell and macropores, $n_\alpha \equiv |Q_\alpha|/|Q|, \alpha = l, f$ and the averaged Darcy's velocity of the fluid in the macropores relative to the solid phase $\widetilde{\boldsymbol{q}_f}^0 \equiv \widetilde{\boldsymbol{v}_f}^0 - n_f \partial \boldsymbol{u}_s^0 / \partial t$. We then have [19]

$$\widetilde{\boldsymbol{q}_f}^0 = -\boldsymbol{K}_F \boldsymbol{\nabla} p_f^0\,,$$

which is the classical Darcy's law governing the macroscopic flow with $\boldsymbol{K}_F$ denoting the permeability coefficient.

Overall Momentum Balance

To derive the overall momentum balance we apply the mean value operator to (16)-(17), use the boundary condition (26) together with (10),(8) to obtain (recall that $\boldsymbol{n}^1$ was chosen outward to Q_l)

$$\begin{aligned}\mathrm{div}_x\widetilde{\boldsymbol{t}}^0 &= \mathrm{div}_x\widetilde{\boldsymbol{t}}_s^{e0} - \boldsymbol{\nabla}_x\widetilde{p}_l{}^0 = -|Q|^{-1}\int_{Q_l}\mathrm{div}_y\boldsymbol{t}^1\,dQ_l = -|Q|^{-1}\int_{\Gamma_1}\boldsymbol{t}^1\boldsymbol{n}^1\,d\Gamma \\ &= -|Q|^{-1}\int_{\Gamma_1}\boldsymbol{t}_f^1\boldsymbol{n}^1\,d\Gamma = |Q|^{-1}\int_{Q_f}\mathrm{div}_y\boldsymbol{t}_f^1\,dQ_f = |Q|^{-1}\int_{Q_f}\boldsymbol{\nabla}_x p_f^0\,dQ_f = n_f\boldsymbol{\nabla}_x p_f^0\end{aligned}$$

where the divergence theorem and periodicity assumptions have also been used. Whence

$$\mathrm{div}_x\widetilde{\boldsymbol{t}}_s^{e0} - \boldsymbol{\nabla}_x\widetilde{p}_l{}^0 - (1-n_l)\boldsymbol{\nabla}_x p_f^0 = 0 \tag{28}$$

The above equation expresses the overall momentum balance. Next, we rewrite (28) in a more convenient form. To this end we define the excess in pore pressure of the cell relative to the macropore system, p_0, and the macroscopic effective stress tensor $\widetilde{\boldsymbol{\sigma}_0}^e$ as

$$\begin{aligned}&p_0 \equiv p_l^0 - p_f^0 \qquad \text{with} \quad \widetilde{p_0} = |Q|^{-1}\int_{Q_l}(p_l^0 - p_f^0)\,dQ_l = \widetilde{p}_l{}^0 - n_l p_f^0 \\ &\boldsymbol{\sigma}_0^e \equiv \boldsymbol{t}_s^{e0} - p_0\boldsymbol{I}\end{aligned} \tag{29}$$

Note from (29) that $\widetilde{\boldsymbol{\sigma}_0}^e$ is not simply the average of microscopic counterpart $\boldsymbol{t}_s^{e0}$ but also incorporates an additional component related to the excess in pore pressure p_0. Using the above definitions we can rewrite (28) in terms of $\{\boldsymbol{\sigma}_0^e, p_f^0\}$

$$\mathrm{div}_x\widetilde{\boldsymbol{\sigma}_0}^e - \boldsymbol{\nabla}_x p_f^0 = 0 \tag{30}$$

If we denote $\widetilde{\boldsymbol{T}}^0$ the overall macroscopic stress tensor, as $\widetilde{\boldsymbol{T}}^0 \equiv \widetilde{\boldsymbol{\sigma}_0}^e - p_f^0\boldsymbol{I}$, the above form of the overall momentum balance resembles in form Terzaghi's decomposition at the macroscale. We now pursue the derivation of an alternative form of writing (30) where the non-oscillatory and fluctuating components of $\boldsymbol{\sigma}_0^e$ appear explicitly decoupled. Recalling that $\boldsymbol{u}_s^0$ depends only on $(\boldsymbol{x}, t)$, from (18) and (29), decompose $\{\boldsymbol{t}_s^{e0}, \boldsymbol{\sigma}_0^e\}$ into their averaged macroscopic and fluctuating components

$$\boldsymbol{t}_s^{e0} = \boldsymbol{\sigma}_0(\boldsymbol{x}, t) + \boldsymbol{\sigma}_1(\boldsymbol{x}, \boldsymbol{y}, t) \tag{31}$$

$$\boldsymbol{\sigma}_0^e = \boldsymbol{\sigma}_0(\boldsymbol{x}, t) + \boldsymbol{\sigma}_1^e(\boldsymbol{x}, \boldsymbol{y}, t) \tag{32}$$

with

$$\boldsymbol{\sigma}_0(\boldsymbol{x}, t) \equiv \lambda_s \mathrm{div}_x \boldsymbol{u}_s^0 \boldsymbol{I} + 2\mu_s \boldsymbol{\nabla}_x^s \boldsymbol{u}_s^0 \tag{33}$$

$$\boldsymbol{\sigma}_1(\boldsymbol{x}, \boldsymbol{y}, t) \equiv \lambda_s \mathrm{div}_y \boldsymbol{u}_s^1 \boldsymbol{I} + 2\mu_s \boldsymbol{\nabla}_y^s \boldsymbol{u}_s^1 \tag{34}$$

$$\boldsymbol{\sigma}_1^e(\boldsymbol{x}, \boldsymbol{y}, t) \equiv \boldsymbol{\sigma}_1 - p_0 \boldsymbol{I}\,. \tag{35}$$

Since $\boldsymbol{\sigma}_0$ is independent of the fast variable $\boldsymbol{y}$, averaging (33) yields

$$\widetilde{\boldsymbol{\sigma}_0} = \lambda_s n_l \mathrm{div}_x \boldsymbol{u}_s^0 \boldsymbol{I} + 2\mu_s n_l \boldsymbol{\nabla}_x^s \boldsymbol{u}_s^0\,.$$

Using the above decompositions in (15) and (17) yields (recall that $\boldsymbol{\sigma}_0 = \boldsymbol{\sigma}_0(\boldsymbol{x}, t)$ and $p_f^0 = p_f^0(\boldsymbol{x}, t)$)

$$\mathrm{div}_y \boldsymbol{t}^0 = \mathrm{div}_y \boldsymbol{t}_s^{e0} - \boldsymbol{\nabla}_y p_l^0 = \mathrm{div}_y \boldsymbol{\sigma}_1 - \boldsymbol{\nabla}_y p_0 = \mathrm{div}_y \boldsymbol{\sigma}_1^e = 0$$

which shows that the fluctuating part of $\boldsymbol{\sigma}_0^e$ satisfies an overall equilibrium equation within each cell. Further, using (32) in (30) gives

$$\mathrm{div}_x \widetilde{\boldsymbol{\sigma}_0} - \boldsymbol{\nabla}_x p_f^0 = -\mathrm{div}_x \widetilde{\boldsymbol{\sigma}_1}^e\,. \tag{36}$$

The above result is the appropriate form of representing the overall momentum balance in a dual porosity formulation. The l.h.s. of (36) contains only global variables (functions of $(\boldsymbol{x}, t)$) whereas the r.h.s. represents a distributed source/sink momentum transfer function from the averaged microscopic system to the global one.

Overall Mass Balance

We now derive the overall macroscopic mass balance. By averaging (13) and (21) using the boundary condition (23) along with the divergence theorem and the periodicity assumption we get

$$n_f \beta_f \frac{\partial p_f^0}{\partial t} + \widetilde{\mathrm{div}_x \boldsymbol{v}_f^0} = -|Q|^{-1} \int_{Q_f} \mathrm{div}_y \boldsymbol{v}_f^1 \, dQ_f = |Q|^{-1} \int_{\Gamma_1} \boldsymbol{v}_f^1 \cdot \boldsymbol{n}^1 \, d\Gamma$$
$$= |Q|^{-1} \int_{\Gamma_1} \left(\boldsymbol{q}_l^1 + \frac{\partial \boldsymbol{u}_s^1}{\partial t} \right) \cdot \boldsymbol{n}^1 \, d\Gamma = |Q|^{-1} \int_{Q_l} \left(\mathrm{div}_y \boldsymbol{q}_l^1 + \mathrm{div}_y \frac{\partial \boldsymbol{u}_s^1}{\partial t} \right) dQ_l$$
$$= -(1 - n_f) \mathrm{div}_x \frac{\partial \boldsymbol{u}_s^0}{\partial t} - \frac{1}{M} \frac{\partial \widetilde{p_l}^0}{\partial t}$$

In terms of the macroscopic Darcy's velocity, $\widetilde{\boldsymbol{q}_f}^0$, the above result gives

$$n_f \beta_f \frac{\partial p_f^0}{\partial t} + \mathrm{div}_x \frac{\partial \boldsymbol{u}_s^0}{\partial t} + \mathrm{div}_x \widetilde{\boldsymbol{q}_f}^0 = -\frac{1}{M} \frac{\partial \widetilde{p_l}^0}{\partial t} \,. \tag{37}$$

Boundary Conditions:

Using (8),(17) and the decomposition (31), boundary condition (25) can be rewritten as

$$-p_f^0 \boldsymbol{n}^1 = \boldsymbol{t}^0 \boldsymbol{n}^1 = (-p_l^0 \boldsymbol{I} + \boldsymbol{t}_s^{e0}) \boldsymbol{n}^1 = (\boldsymbol{\sigma}_0 + \boldsymbol{\sigma}_1 - p_l^0 \boldsymbol{I}) \boldsymbol{n}^1 \quad \text{on} \quad \Gamma_1 \,. \tag{38}$$

Together with boundary condition (27), this yields

$$\boldsymbol{\sigma}_1 \boldsymbol{n}^1 = -\boldsymbol{\sigma}_0 \boldsymbol{n}^1 \quad \text{on} \quad \Gamma_1 \tag{39}$$

Denoting Γ_0 the macroscopic boundary of the reservoir with unit outward normal $\boldsymbol{n}^0$ and $\{\Gamma_0^1, \Gamma_0^2\}$ disjoint subsets of Γ_0 $(\Gamma_0^1 \cup \Gamma_0^2 = \Gamma_0)$, postulate the following macroscopic boundary conditions

$$\boldsymbol{u}_s^0 = 0 \,, \quad \boldsymbol{q}_f^0 \cdot \boldsymbol{n}^0 = 0 \quad \text{on} \quad \Gamma_0^1$$
$$p_f^0 = 0 \,, \quad \widetilde{\boldsymbol{\sigma}_0}^e \boldsymbol{n}^0 = \boldsymbol{h} \quad \text{on} \quad \Gamma_0^2$$

Here the boundaries Γ_0^1 and Γ_0^2 correspond to impervious rigid and permeable walls with free drainage respectively. The function $\boldsymbol{h}$ denotes a traction boundary condition for the mechanical problem.

Summary of the Dual Porosity Model

Let $\lambda_S \equiv \lambda_s n_l$, $\mu_S \equiv n_l \mu_s$ and $\beta \equiv \beta_f n_f$. Application of the formal homogenization procedure leads to the following dual porosity model: Find

$\{\boldsymbol{u}_s^0, \widetilde{\boldsymbol{\sigma}}_0, p_f^0, \widetilde{\boldsymbol{q}_f}^0\}$ functions of $(\boldsymbol{x}, t)$ and $\{p_l^0, \boldsymbol{\sigma}_1^e, \boldsymbol{u}_s^1, \boldsymbol{q}_l^1, \boldsymbol{\sigma}_1\}$ functions of $(\boldsymbol{x}, \boldsymbol{y}, t)$ such that

$$\left\{\begin{array}{ll} \mathrm{div}_x \widetilde{\boldsymbol{\sigma}}_0 - \boldsymbol{\nabla}_x p_f^0 = \boldsymbol{F}_*(\boldsymbol{x}, t) & \\ \widetilde{\boldsymbol{\sigma}}_0 = \lambda_S \mathrm{div}_x \boldsymbol{u}_s^0 \boldsymbol{I} + 2\mu_S \boldsymbol{\nabla}_x^s \boldsymbol{u}_s^0 & \\ \beta \dfrac{\partial p_f^0}{\partial t} + \mathrm{div}_x \widetilde{\boldsymbol{q}_f}^0 + \mathrm{div}_x \dfrac{\partial \boldsymbol{u}_s^0}{\partial t} = G_*(\boldsymbol{x}, t) & \\ \widetilde{\boldsymbol{q}_f}^0 = -\boldsymbol{K}_F \boldsymbol{\nabla}_x p_f^0 & \boldsymbol{x} \in \Omega, t > 0 \end{array}\right. \tag{40}$$

with

$$\boldsymbol{F}_* \equiv -\frac{1}{|Q|} \mathrm{div}_x \int_{Q_l} \boldsymbol{\sigma}_1^e \, dQ_l, \quad G_* \equiv -\frac{1}{M|Q|} \int_{Q_l} \frac{\partial p_l^0}{\partial t} \, dQ_l$$

and

$$\left\{\begin{array}{ll} \mathrm{div}_y \boldsymbol{\sigma}_1^e = 0 & \\ \boldsymbol{\sigma}_1^e = -(p_l^0 - p_f^0(\boldsymbol{x}, t))\boldsymbol{I} + \boldsymbol{\sigma}_1 & \\ \boldsymbol{\sigma}_1 = \lambda_s \mathrm{div}_y \boldsymbol{u}_s^1 + 2\mu_s \boldsymbol{\nabla}_y^s \boldsymbol{u}_s^1 & \\ \dfrac{1}{M} \dfrac{\partial p_l^0}{\partial t} + \mathrm{div}_y \boldsymbol{q}_l^1 + \mathrm{div}_y \dfrac{\partial \boldsymbol{u}_s^1}{\partial t} = -\mathrm{div}_x \dfrac{\partial \boldsymbol{u}_x^0}{\partial t}(\boldsymbol{x}, t) & \\ \boldsymbol{q}_l^1 = -K_l \boldsymbol{\nabla}_y p_l^0 & \boldsymbol{y} \in Q_l, t > 0 \end{array}\right. \tag{41}$$

supplemented by boundary and initial conditions

$$\left\{\begin{array}{l} \boldsymbol{\sigma}_1 \boldsymbol{n}^1 = -\boldsymbol{\sigma}_0 \boldsymbol{n}^1 \quad \text{on} \quad \Gamma_1 \\ p_l^0 = p_f^0 \quad \text{on} \quad \Gamma_1 \\ \boldsymbol{u}_s^0 = 0\,, \quad \boldsymbol{q}_f^0 \cdot \boldsymbol{n}^0 = 0 \quad \text{on} \quad \Gamma_0^1 \\ p_f^0 = 0\,, \quad \widetilde{\boldsymbol{\sigma}}_0{}^e \boldsymbol{n}^0 = \boldsymbol{h} \quad \text{on} \quad \Gamma_0^2 \\ \mathrm{div}_x \boldsymbol{u}_s^0 = \mathrm{div}_y \boldsymbol{u}_s^1 = 0, \quad t = 0\,, \\ p_l^0 = p_f^0 = \overline{p}, \quad t = 0\,, \end{array}\right. \tag{42}$$

with the macroscopic effective stress tensor given as $\widetilde{\boldsymbol{\sigma}}_0{}^e = \widetilde{\boldsymbol{\sigma}}_0 + \widetilde{\boldsymbol{\sigma}}_1 - (\widetilde{p}_l{}^0 - \widetilde{p_f}{}^0)\boldsymbol{I}$. The above homogenized results lead to a macrostructure model of dual porosity type, wherein the reservoir is represented by two overlapping continua: one representing the global macroscopic transport equations (eq. (40)) and the other the local cell problems at the microscale (eq. (41)). For each point of the macroscopic domain is identified a magnified or scaled local cell Q which is coupled to the global problem via the distributed source/sink momentum and mass transfer functions $\boldsymbol{F}_*$ and G_*.

Let $\beta' \equiv \beta + n_l/M$. In terms of $\{\boldsymbol{u}_s^0, p_f^0\}$ and $\{\boldsymbol{u}_s^1, p_0\}$ the above system can be rewritten as

$$\left\{\begin{array}{ll} \mu_S \triangle_{xx} \boldsymbol{u}_s^0 + (\lambda_S + \mu_S) \boldsymbol{\nabla}_x \mathrm{div}_x \boldsymbol{u}_s^0 - \boldsymbol{\nabla}_x p_f^0 = \boldsymbol{F}_* & \\ \beta' \dfrac{\partial p_f^0}{\partial t} + \mathrm{div}_x \dfrac{\partial \boldsymbol{u}_s^0}{\partial t} - \mathrm{div}_x(\boldsymbol{K}_F \boldsymbol{\nabla}_x p_f^0) = G'_* & \boldsymbol{x} \in \Omega, t > 0 \end{array}\right. \tag{43}$$

with

$$\left\{\begin{array}{l} \boldsymbol{F}_*(\boldsymbol{x},t) = -2\mu_s \mathrm{div}_x \widetilde{\boldsymbol{\nabla}_y^s \boldsymbol{u}_s^1} - \lambda_s \boldsymbol{\nabla}_x \widetilde{\mathrm{div}_y \boldsymbol{u}_s^1} + \boldsymbol{\nabla}_x \widetilde{p_0} \\ G'_* = -\dfrac{1}{M}\dfrac{\partial \widetilde{p_0}}{\partial t} \end{array}\right. \tag{44}$$

and

$$\left\{\begin{array}{ll} \mu_s \triangle_{yy} \boldsymbol{u}_s^1 + (\lambda_s + \mu_s)\boldsymbol{\nabla}_y \mathrm{div}_y \boldsymbol{u}_s^1 - \boldsymbol{\nabla}_y p_0 = 0 & \boldsymbol{y} \in Q_l, t > 0 \\ \dfrac{1}{M}\dfrac{\partial p_0}{\partial t} + \mathrm{div}_y \dfrac{\partial \boldsymbol{u}_s^1}{\partial t} - K_l \triangle_{yy} p_0 = -\mathrm{div}_x \dfrac{\partial \boldsymbol{u}_s^0}{\partial t}(\boldsymbol{x},t) - \dfrac{1}{M}\dfrac{\partial p_f^0}{\partial t}(\boldsymbol{x},t) & \end{array}\right. \tag{45}$$

If we rewrite boundary and initial conditions in terms of p_0, the second and last equations in (42) give

$$p_0 = 0 \quad \text{on} \quad \Gamma_1 \quad \text{and} \quad p_0 = 0, \quad \text{in} \quad Q_l, t = 0 \tag{46}$$

The case where the fluids in the macro and micropores are incompressible can easily be reproduced by setting $M \to \infty$ and $\beta' \to 0$ in (43)-(46). This leads to the following incompressible fluid system

$$\left\{\begin{array}{l} \mu_S \triangle_{xx} \boldsymbol{u}_s^0 + (\lambda_S + \mu_S)\boldsymbol{\nabla}_x \mathrm{div}_x \boldsymbol{u}_s^0 - \boldsymbol{\nabla}_x p_f^0 = \boldsymbol{F}_* \\ \mathrm{div}_x \dfrac{\partial \boldsymbol{u}_s^0}{\partial t} - \mathrm{div}(\boldsymbol{K}_F \boldsymbol{\nabla}_x p_f^0) = 0 \\ \boldsymbol{F}_* = -\mathrm{div}_x \widetilde{\boldsymbol{\sigma}_1}^e = -2\mu_s \mathrm{div}_x \widetilde{\boldsymbol{\nabla}_y^s \boldsymbol{u}_s^1} - \lambda_s \boldsymbol{\nabla}_x \widetilde{\mathrm{div}_y \boldsymbol{u}_s^1} + \boldsymbol{\nabla}_x \widetilde{p_0} \qquad \boldsymbol{x} \in \Omega, t > 0 \end{array}\right. \tag{47}$$

and

$$\left\{\begin{array}{ll} \mu_s \triangle_{yy} \boldsymbol{u}_s^1 + (\lambda_s + \mu_s)\boldsymbol{\nabla}_y \mathrm{div}_y \boldsymbol{u}_s^1 - \boldsymbol{\nabla}_y p_0 = 0 & \\ \mathrm{div}_y \dfrac{\partial \boldsymbol{u}_s^1}{\partial t} - K_l \triangle_{yy} p_0 = -\mathrm{div}_x \dfrac{\partial \boldsymbol{u}_s^0}{\partial t}(\boldsymbol{x},t) & \boldsymbol{y} \in Q_l, t > 0 \end{array}\right. \tag{48}$$

In this case, the distributed mass transfer function G_* vanishes and consequently the local system influences the global one only through the momentum transfer function $\boldsymbol{F}_*$.

Equivalence with Volterra Integrodifferential Equations

The well posedness and analysis of the above microstructural model of dual porosity type can be obtained by exploiting the equivalence with Volterra Integrodifferential equations. It has been shown by Arbogast [2] (for rigid solid phase) and Murad and Cushman [13] (for deformable porous matrix) that application of the Green's function method leads to an explicit decoupling between local and global equations and reduces the dual porosity model to a system of integrodifferential equation of Volterra type, where the dependence on the microstructure (represented by the distributed source terms $\boldsymbol{F}_*$ and G_* in (47)) is replaced by convolution terms with kernels describing the fading memory effects (see [3, 10, 15, 16]). The physics underlying the appearance of memory effects is tied directly to the difference between the time scales inherent to the flows in the micro and macro-pore systems, i.e. the delay effect caused by the slower flow in the micro pores which is manifested in the convolution kernels. The equivalence between dual porosity models and Volterra equations with memory allows to apply the established techniques of analysis of integrodifferential equations (based on e.g. strongly positive kernels see e.g. [9]) to show well-posedness of the homogenized dual porosity model. In the particular case of deformable media, Murad and Cushman [13] also showed that the integrodifferential equations resultant from application of the Greens function method resembles in form the Volterra equation of second kind which commonly appear in hereditary viscoelasticity, where stresses are represented in terms of the functionals of the strain history (see [13]).

4. Variational Formulation

We shall henceforth discuss the numerical solution of the incompressible microstructural model (47),(48). To this end denote respectively $L^2(\Omega)$ and $L^2(Q_l)$ the usual Sobolev spaces of square integrable global and local (periodic) scalar functions defined on Ω and Q_l with inner products

$$\begin{aligned}\Big(f,g\Big)_0 &\equiv \int_\Omega f\,g\,d\Omega \quad \forall f,g\in L^2(\Omega)\\ \Big(f,g\Big)_1 &\equiv \int_{Q_l} f\,g\,dQ_l \quad \forall f,g\in L^2(Q_l)\,.\end{aligned}$$

Further denote respectively $H^1(\Omega)$ and $H^1(Q_l)$ the Sobolev subspaces of $L^2(\Omega)$ and $L^2(Q_l)$ consisting of functions with the derivatives $\partial\boldsymbol{f}$ and $\partial\boldsymbol{g}$ satisfying

$\{\partial \boldsymbol{f}, \partial \boldsymbol{g}\} \in L^2(\Omega) \times L^2(Q_l)$ in the usual distributional sense. Define the global spaces $\boldsymbol{U}^0 \times V^0$ for $\{\boldsymbol{u}_s^0, p_f^0\}$ and the local spaces $\boldsymbol{U}^1 \times V^1$ for $\{\boldsymbol{u}_s^1, p_0\}$ as

$$\begin{aligned}
&\boldsymbol{U}^0 \equiv \{\boldsymbol{v}^0 \in (H^1(\Omega))^3, \quad \boldsymbol{v}^0 = \boldsymbol{0} \quad \text{on} \quad \Gamma_0^1\} \\
&V^0 \equiv \{q^0 \in H^1(\Omega), \quad q^0 = 0 \quad \text{on} \quad \Gamma_0^2\} \\
&\boldsymbol{U}^1 = \{\boldsymbol{v}^1 \in (H^1(Q_l))^3, \quad \int_{Q_l} \boldsymbol{v}^1 \, dQ_l = 0\} \\
&V^1 \equiv H_0^1(Q_l) \equiv \{q^1 \in H^1(Q_l), \quad q^1 = 0 \quad \text{on} \quad \Gamma_1\}
\end{aligned}$$

Introduce the bilinear forms

$$\begin{aligned}
a_x(\boldsymbol{u}_s^0, \boldsymbol{v}^0) &= \Big(\boldsymbol{c}_S \boldsymbol{\varepsilon}_x(\boldsymbol{u}_s^0), \boldsymbol{\varepsilon}_x(\boldsymbol{v}^0)\Big)_0 = 2\mu_S \Big(\boldsymbol{\varepsilon}_x(\boldsymbol{u}_s^0), \boldsymbol{\varepsilon}_x(\boldsymbol{v}^0)\Big)_0 + \lambda_S \Big(\mathrm{div}_x \boldsymbol{u}_s^0, \mathrm{div}_x \boldsymbol{v}^0\Big)_0 \\
a_y(\boldsymbol{u}_s^1, \boldsymbol{v}^1) &= \Big(\boldsymbol{c}_s \boldsymbol{\varepsilon}_y(\boldsymbol{u}_s^1), \boldsymbol{\varepsilon}_y(\boldsymbol{v}^1)\Big)_1 = 2\mu_s \Big(\boldsymbol{\varepsilon}_y(\boldsymbol{u}_s^1), \boldsymbol{\varepsilon}_y(\boldsymbol{v}^1)\Big)_1 + \lambda_s \Big(\mathrm{div}_y \boldsymbol{u}_s^1, \mathrm{div}_y \boldsymbol{v}^1\Big)_1 \\
d_x(p_f^0, q^0) &= \Big(\boldsymbol{K}_F \boldsymbol{\nabla}_x p_f^0, \boldsymbol{\nabla}_x q^0\Big)_0 \\
d_y(p_0, q^1) &= K_l \Big(\boldsymbol{\nabla}_y p_0, \boldsymbol{\nabla}_y q^1\Big)_1,
\end{aligned}$$

where $\boldsymbol{\varepsilon}_x(\boldsymbol{u}) \equiv \boldsymbol{\nabla}_x^s(\boldsymbol{u})$ and $\boldsymbol{\varepsilon}_y(\boldsymbol{u}) \equiv \boldsymbol{\nabla}_y^s(\boldsymbol{u})$. Making use of (32), the variational formulation for (47)-(48) consists in: For each $t \in (0, \infty)$, find the pairs $\{\boldsymbol{u}_s^0, p_f^0\} \in \boldsymbol{U}^0 \times V^0$ and $\{\boldsymbol{u}_s^1, p_0\} \in \boldsymbol{U}^1 \times V^1$ such that:

$$\begin{aligned}
a_x(\boldsymbol{u}_s^0, \boldsymbol{v}^0) - (p_f^0, \mathrm{div}_x \boldsymbol{v}^0)_0 &= F(\{\widetilde{\boldsymbol{u}_s}^1, \widetilde{p_0}\}; \boldsymbol{v}^0) + f(\boldsymbol{v}^0) \quad \forall \boldsymbol{v}^0 \in \boldsymbol{U}^0 \\
(\mathrm{div}_x \frac{\partial \boldsymbol{u}_s^0}{\partial t}, q^0)_0 + d_x(p_f^0, q^0) &= 0 \quad \forall q^0 \in V^0
\end{aligned} \tag{49}$$

and

$$\begin{aligned}
a_y(\boldsymbol{u}_s^1, \boldsymbol{v}^1) - (p_0, \mathrm{div}_y \boldsymbol{v}^1)_1 &= L(\boldsymbol{\sigma}_0; \boldsymbol{v}^1) \quad \forall \boldsymbol{v}^1 \in \boldsymbol{U}^1 \\
(\mathrm{div}_y \frac{\partial \boldsymbol{u}_s^1}{\partial t}, q^1)_1 + d_y(p_0, q^1) &= -(\mathrm{div}_x \frac{\partial \boldsymbol{u}_s^0}{\partial t}, q^1)_1 \quad \forall q^1 \in V^1
\end{aligned} \tag{50}$$

with

$$\begin{aligned}
&F(\{\widetilde{\boldsymbol{u}_s}^1, \widetilde{p_0}\}; \boldsymbol{v}^0) = -\Big(\widetilde{\boldsymbol{\sigma}_1}^e, \boldsymbol{\varepsilon}_x(\boldsymbol{v}^0)\Big)_0 = -\Big(\boldsymbol{c}_s \widetilde{\boldsymbol{\varepsilon}_y}(\boldsymbol{u}_s^1), \boldsymbol{\varepsilon}_x(\boldsymbol{v}^0)\Big)_0 + \Big(\widetilde{p_0}, \mathrm{div}_x \boldsymbol{v}^0\Big)_0, \\
&f(\boldsymbol{v}^0) = \int_{\Gamma_0^2} \widetilde{\boldsymbol{\sigma}_0}^e \boldsymbol{n}^0 \cdot \boldsymbol{v}^0 \, d\Gamma = \int_{\Gamma_0^2} \boldsymbol{h} \cdot \boldsymbol{v}^0 \, d\Gamma \\
&L(\boldsymbol{\sigma}_0; \boldsymbol{v}^1) = -\int_{\Gamma_1} \boldsymbol{\sigma}_0 \boldsymbol{n}^1 \cdot \boldsymbol{v}^1 \, d\Gamma \\
&(\mathrm{div}_x \boldsymbol{u}_s^0, q^0)_0 = (\mathrm{div}_y \boldsymbol{u}_s^1, q^1)_1 = 0 \quad \forall \{q^0, q^1\} \quad \text{in} \quad V^0 \times V^1,\ t = 0
\end{aligned}$$

4.1. Time Stepping

We now discretize the above variational formulation in the time domain by the backward Euler method. Denote n≥ 1 an integer number and let Δt be a fixed time step (assumed the same for both local and global problems). The backward Euler method seeks a solution $\boldsymbol{u}^n$ at time $t_n = n\Delta t$ by replacing the time derivative $\partial \boldsymbol{u}/\partial t$ by the backward difference quotient $\partial_t \boldsymbol{u}^n = (\boldsymbol{u}^n - \boldsymbol{u}^{n-1})/\Delta t$. Let $\{\boldsymbol{u}_0^n, p_f^n\}$ and $\{\boldsymbol{u}_1^n, p_0^n\}$ be the approximations of $\{\boldsymbol{u}_s^0, p_f^0\}$ and $\{\boldsymbol{u}_s^1, p_0\}$ at time $t_n = n\Delta t$ respectively, satisfying the following semidiscrete version of (49) and (50): For each time step $n\Delta t$, $n \geq 1$, find the pairs $\{\boldsymbol{u}_0^n, p_f^n\} \in \boldsymbol{U}^0 \times V^0$ and $\{\boldsymbol{u}_1^n, p_0^n\} \in \boldsymbol{U}^1 \times V^1$ such that

$$\begin{aligned} a_x(\boldsymbol{u}_0^n, \boldsymbol{v}^0) - (p_f^n, \mathrm{div}_x \boldsymbol{v}^0)_0 &= F^n(\{\widetilde{\boldsymbol{u}_1}^n, \widetilde{p_0}^n\}; \boldsymbol{v}^0) + f(\boldsymbol{v}^0) \quad \forall \boldsymbol{v}^0 \in \boldsymbol{U}^0 \\ (\mathrm{div}_x \boldsymbol{u}_0^n, q^0)_0 + \Delta t\, d_x(p_f^n, q^0) &= (\mathrm{div}_x \boldsymbol{u}_0^{n-1}, q^0)_0 \qquad \forall q^0 \in V^0 \end{aligned} \tag{51}$$

and

$$\begin{aligned} a_y(\boldsymbol{u}_1^n, \boldsymbol{v}^1) &- (p_0^n, \mathrm{div}_y \boldsymbol{v}^1)_1 = L^n(\boldsymbol{\sigma}_0^n, \boldsymbol{v}^1) \quad \forall \boldsymbol{v}^1 \in \boldsymbol{U}^1 \\ (\mathrm{div}_y \boldsymbol{u}_1^n, q^1)_1 + \Delta t\, d_y(p_0^n, q^1) &= (\mathrm{div}_y \boldsymbol{u}_1^{n-1}, q^1)_1 - (\mathrm{div}_x(\boldsymbol{u}_0^n - \boldsymbol{u}_0^{n-1}), q^1)_1 \\ &\qquad \forall q^1 \in V^1 \end{aligned} \tag{52}$$

with

$$\begin{aligned} & F^n(\{\widetilde{\boldsymbol{u}_1}^n, \widetilde{p_0}^n\}; \boldsymbol{v}^0) = -(\widetilde{\boldsymbol{\sigma}_1}^{en}, \boldsymbol{\varepsilon}_x(\boldsymbol{v}^0))_0 \\ & L^n(\boldsymbol{\sigma}_0^n, \boldsymbol{v}^1) = -\int_{\Gamma_1} \boldsymbol{\sigma}_0^n \boldsymbol{n}^1 \cdot \boldsymbol{v}^1 \, d\Gamma \\ & (\mathrm{div}_x \boldsymbol{u}_0^0, q^0)_0 = (\mathrm{div}_y \boldsymbol{u}_1^0, q^1)_1 = 0, \qquad t = 0 \end{aligned} \tag{53}$$

To solve the above problem we exploit the linearity between $\{\boldsymbol{u}_1^n, p_0^n\}$ and the global source terms in the local cell problem (52) (terms involving $\{-\boldsymbol{\sigma}_0^n, -\mathrm{div}_x \boldsymbol{u}_0^n$ and $\mathrm{div}_x \boldsymbol{u}_0^{n-1}\}$ depending on $(\boldsymbol{x}, t)$). To this end, we define the pair of characteristic functions $\{\boldsymbol{\chi}^{\boldsymbol{u}}, \chi^p\}$ depending on $\boldsymbol{y}$ satisfying

$$\begin{aligned} a_y(\boldsymbol{\chi}^{\boldsymbol{u}}, \boldsymbol{v}^1) - (\chi^p, \mathrm{div}_y \boldsymbol{v}^1)_1 = 0 \quad \forall \boldsymbol{v}^1 \in \boldsymbol{U}^1 \\ (\mathrm{div}_y \boldsymbol{\chi}^{\boldsymbol{u}}, q^1)_1 + \Delta t\, d_y(\chi^p, q^1) = -(1, q^1)_1 \quad \forall q^1 \in V^1 . \end{aligned} \tag{54}$$

For a fixed time step, $\{\boldsymbol{\chi}^{\boldsymbol{u}}, \chi^p\}$ may be interpreted as purely geometric quantities, representing the solution of the cell due to an unitary change in the fluid content. In addition, denoting $\otimes$ the tensorial product between vectors, and $\{\boldsymbol{e}_k\}$,$(k = 1, 2, 3)$ an orthonormal basis where the identity is represented as $\delta_{ij} = \boldsymbol{e}_i \otimes \boldsymbol{e}_j$, define the pair of third and second rank tensorial characteristic functions $\{\boldsymbol{\chi}^{\boldsymbol{U}}, \boldsymbol{\chi}^{\boldsymbol{P}}\}$ whose components $\{\chi^U_{kij}, \chi^P_{ij}\}$ (or using vectorial notation $\{\boldsymbol{\chi}^{\boldsymbol{U}}_{ij}, \chi^P_{ij}\}$ with $\boldsymbol{\chi}^{\boldsymbol{U}}_{ij} \equiv \chi^U_{kij}$) satisfy the following elliptic problems

$$
\begin{aligned}
a_y(\boldsymbol{\chi}^{\boldsymbol{U}}_{ij}, \boldsymbol{v}^1) - (\chi^P_{ij}, \mathrm{div}_y \boldsymbol{v}^1)_1 = L_{ij}(\boldsymbol{v}^1) \quad \forall \boldsymbol{v}^1 \in \boldsymbol{U}^1 \\
(\mathrm{div}_y \boldsymbol{\chi}^{\boldsymbol{U}}_{ij}, q^1)_1 + \Delta t \, d_y(\chi^P_{ij}, q^1) = 0 \quad \forall q^1 \in V^1, \qquad i, j = 1, 2, 3
\end{aligned}
\tag{55}
$$

with

$$
L_{ij}(\boldsymbol{v}^1) = -\int_{\Gamma_1} \boldsymbol{I}\boldsymbol{I}\boldsymbol{n}^1 \cdot \boldsymbol{v}^1 \, d\Gamma = -\int_{\Gamma_1} \delta_{ij}\delta_{kl} n_l v_k \, d\Gamma = -\int_{\Gamma_1} (\boldsymbol{e}_i \otimes \boldsymbol{e}_j) n_k v_k \, d\Gamma \tag{56}
$$

where $\{n_k, v_k\}$ are the components of $\{\boldsymbol{n}^1, \boldsymbol{v}^1\}$ on the basis $\boldsymbol{e}_k$. Physically, these characteristic deformations represent the nearly incompressible response of the cell due to unitary traction boundary conditions.

Finally, define the pair $\{\boldsymbol{u}^n_*, p^n_*\} \in \boldsymbol{U}^1 \times V^1$ satisfying the evolution problem

$$
\begin{aligned}
a_y(\boldsymbol{u}^n_*, \boldsymbol{v}^1) \quad &- \quad (p^n_*, \mathrm{div}_y \boldsymbol{v}^1)_1 = 0 \quad \forall \boldsymbol{v}^1 \in \boldsymbol{U}^1 \\
(\mathrm{div}_y \boldsymbol{u}^n_*, q^1)_1 + \Delta t \, d_y(p^n_*, q^1) \quad &= \quad (\mathrm{div}_y \boldsymbol{u}^{n-1}_1 + \mathrm{div}_x \boldsymbol{u}^{n-1}_0, q^1)_1 \quad \forall q^1 \in V^1
\end{aligned}
\tag{57}
$$

with $(\mathrm{div}_y \boldsymbol{u}^0_1, q^1)_1 = (\mathrm{div}_x \boldsymbol{u}^0_0, q^1)_1 = 0$. The above variational formulation can be viewed as a reduced form of (52) where the r.h.s. involves only terms in the previous time $t_{n-1} = (n-1)\Delta t$. By invoking the linearity between (52) and (54)–(57) we have

$$
\boldsymbol{u}^n_1 = \boldsymbol{u}^n_* + (\mathrm{div}_x \boldsymbol{u}^n_0)\boldsymbol{\chi}^{\boldsymbol{u}} + \boldsymbol{\chi}^{\boldsymbol{U}} : \boldsymbol{\sigma}^n_0 \tag{58}
$$

$$
p^n_0 = p^n_* + (\mathrm{div}_x \boldsymbol{u}^n_0)\chi^p + \boldsymbol{\chi}^{\boldsymbol{P}} : \boldsymbol{\sigma}^n_0 \, . \tag{59}
$$

For a given solution $\{\boldsymbol{u}^n_0, p^n_f\}$ of the global problem, the above decompositions provide an alternative procedure to obtain $\{\boldsymbol{u}^n_1, p^n_0\}$. The terms in the r.h.s. of (58) and (59) can be easily determined. For a fixed time step the characteristic functions are purely geometric quantities satisfying the elliptic problems (54)-(56) and only need to be evaluated once. The r.h.s. of the reduced evolutionary problem (57) contains information only on the previous time t_{n-1} and therefore can easily be implemented in conjunction with any step-by-step algorithm. Using (58) and (59) in (34) and (35) one can compute $\boldsymbol{\sigma}_1^e$ at time $t = t_n$

$$\begin{aligned}\widetilde{\boldsymbol{\sigma}_1}^{en} &= -\widetilde{p_0}^n \boldsymbol{I} + \boldsymbol{c}_s \widetilde{\boldsymbol{\varepsilon}_y}(\boldsymbol{u}_1^n) = -\widetilde{p_*}^n \boldsymbol{I} \\ &+ \boldsymbol{c}_s \widetilde{\boldsymbol{\varepsilon}_y}(\boldsymbol{u}_*^n) + \mathrm{div}_x \boldsymbol{u}_0^n \Big(\boldsymbol{c}_s \widetilde{\boldsymbol{\chi}_0}^{\boldsymbol{u}} - \widetilde{\chi}^p \boldsymbol{I} \Big) + \widetilde{\boldsymbol{\chi}_0}^{\boldsymbol{U}} \boldsymbol{c}_s \boldsymbol{\varepsilon}_x(\boldsymbol{u}_0^n) - \widetilde{\boldsymbol{\chi}}^{\boldsymbol{P}} : \boldsymbol{c}_s \boldsymbol{\varepsilon}_x(\boldsymbol{u}_0^n) \boldsymbol{I}\end{aligned}$$

where $\boldsymbol{\chi}_0^{\boldsymbol{u}} \equiv \boldsymbol{\varepsilon}_y(\boldsymbol{\chi}^{\boldsymbol{u}})$ and $\boldsymbol{\chi}_0^{\boldsymbol{U}} \equiv \boldsymbol{c}_s \boldsymbol{\varepsilon}_y(\boldsymbol{\chi}^{\boldsymbol{U}})$ are second and fourth rank tensorial quantities and constitutive relation (33) was used to eliminate $\boldsymbol{\sigma}_0^n$. Using the above result in (53), for fixed characteristic functions one can decompose the linear functional F^n as follows

$$F^n(\{\widetilde{\boldsymbol{u}_1}^n, \widetilde{p_0}^n\}, \boldsymbol{v}^0) = F_1^n(\boldsymbol{u}_0^n, \boldsymbol{v}^0) + F_2^n(\{\widetilde{\boldsymbol{u}_*}^n, \widetilde{p_*}^0\}, \boldsymbol{v}^0)$$

$$F_2^n(\{\widetilde{\boldsymbol{u}_*}^n, \widetilde{p_*}^n\}, \boldsymbol{v}^0) \equiv -\Big(\boldsymbol{c}_s \widetilde{\boldsymbol{\varepsilon}_y}(\boldsymbol{u}_*^n), \boldsymbol{\varepsilon}_x(\boldsymbol{v}^0) \Big)_0 + \Big(\widetilde{p_*}^n, \mathrm{div}_x \boldsymbol{v}^0 \Big)_0$$

$$\begin{aligned}F_1^n(\boldsymbol{u}_0^n, \boldsymbol{v}^0) \equiv &-\Big(\widetilde{\boldsymbol{\chi}_0}^{\boldsymbol{U}} \boldsymbol{c}_s \boldsymbol{\varepsilon}_x(\boldsymbol{u}_0^n) + \mathrm{div}_x \boldsymbol{u}_0^n \boldsymbol{c}_s \widetilde{\boldsymbol{\chi}_0}^{\boldsymbol{u}}, \boldsymbol{\varepsilon}_x(\boldsymbol{v}^0) \Big)_0 \\ &+ \Big((\widetilde{\boldsymbol{\chi}}^{\boldsymbol{P}} : \boldsymbol{c}_s \boldsymbol{\varepsilon}_x(\boldsymbol{u}_0^n) + \widetilde{\chi}^p) \mathrm{div}_x \boldsymbol{u}_0^n, \mathrm{div}_x \boldsymbol{v}^0 \Big)_0\end{aligned}$$

Further, using the above decompositions in (51) gives

$$\begin{aligned}&a_x^*(\boldsymbol{u}_0^n, \boldsymbol{v}^0) - (p_f^n, \mathrm{div}_x \boldsymbol{v}^0)_0 = F_2^n(\{\widetilde{\boldsymbol{u}_*}^n, \widetilde{p_*}^n\}, \boldsymbol{v}^0) + f(\boldsymbol{v}^0) \quad \forall \boldsymbol{v}^0 \in \boldsymbol{U}^0 \\ &(\mathrm{div}_x \boldsymbol{u}_0^n, q^0)_0 + \Delta t \, d_x(p_f^n, q^0) = (\mathrm{div}_x \boldsymbol{u}_0^{n-1}, q^0)_0 \qquad \forall q^0 \in V^0\end{aligned} \tag{60}$$

where $a_x^*(\boldsymbol{u}_0^n, \boldsymbol{v}^0)$ denotes a modified bilinear form defined as

$$\begin{aligned}a_x^*(\boldsymbol{u}_0^n, \boldsymbol{v}^0) \equiv a_x(\boldsymbol{u}_0^n, \boldsymbol{v}^0) - F_1^n(\boldsymbol{u}_0^n, \boldsymbol{v}^0) = \Big((\widetilde{\boldsymbol{\chi}_0}^{\boldsymbol{U}} + n_l \boldsymbol{I}\boldsymbol{I}) \boldsymbol{c}_s \boldsymbol{\varepsilon}_x(\boldsymbol{u}_0^n), \boldsymbol{\varepsilon}_x(\boldsymbol{v}^0) \Big)_0 \quad (61) \\ + \Big(\boldsymbol{c}_s \widetilde{\boldsymbol{\chi}_0}^{\boldsymbol{u}} \mathrm{div}_x \boldsymbol{u}_0^n, \boldsymbol{\varepsilon}_x(\boldsymbol{v}^0) \Big)_0 - \Big((\widetilde{\boldsymbol{\chi}}^{\boldsymbol{P}} : \boldsymbol{c}_s \boldsymbol{\varepsilon}_x(\boldsymbol{u}_0^n) + \widetilde{\chi}^p) \mathrm{div}_x \boldsymbol{u}_0^n, \mathrm{div}_x \boldsymbol{v}^0 \Big)_0\end{aligned}$$

Hence, we can formulate the following backward-Euler semidiscrete problem related to (51)-(53)

Problem M: For $\{\boldsymbol{\chi}^{\boldsymbol{u}}, \boldsymbol{\chi}^{p}\}$ and $\{\boldsymbol{\chi}^{\boldsymbol{U}}, \boldsymbol{\chi}^{\boldsymbol{P}}\}$ solutions of (54) and (55), find, for each time step $n\Delta t$, $n \geq 1$, the pairs $\{\boldsymbol{u}_*^n, p_*^n\} \in \boldsymbol{U}^1 \times V^1$ and $\{\boldsymbol{u}_0^n, p_f^n\} \in \boldsymbol{U}^0 \times V^0$ satisfying (57) and (60) respectively.

4.2. Finite Element Approximation

We now turn to the approximate solution of Problem M by finite elements. Let $\{\boldsymbol{U}_h^0, V_h^0\}$ and $\{\boldsymbol{U}_h^1, V_h^1\}$ be families of finite dimensional subspaces of $\{\boldsymbol{U}^0, V^0\}$ and $\{\boldsymbol{U}^1, V^1\}$. We may think of $\{\boldsymbol{U}_h^0, V_h^0\}$ and $\{\boldsymbol{U}_h^1, V_h^1\}$ as containing continuous, piecewise polynomials of degrees $\{k^0, l^0\}$ and $\{k^1, l^1\}$ on elements of partitions of Ω and Q_l respectively. Let the pairs $\{\boldsymbol{\chi}_h^{\boldsymbol{u}}, \chi_h^p\}$ and $\{\boldsymbol{\chi}_{ijh}^{\boldsymbol{U}}, \chi_{ijh}^P\} \in \boldsymbol{U}_h^1 \times V_h^1$ be the finite element approximations of $\{\boldsymbol{\chi}^{\boldsymbol{u}}, \chi^p\}$ and $\{\boldsymbol{\chi}_{ij}^{\boldsymbol{U}}, \chi_{ij}^P\}$ satisfying theg discrete versions of (54) and (55). In addition let $\{\boldsymbol{u}_{0h}^n, p_{fh}^n\} \in \boldsymbol{U}_h^0 \times V_h^0$, $\{\boldsymbol{u}_{1h}^n, p_{0h}^n\}$ and $\{\boldsymbol{u}_{*h}^n, p_{*h}^n\} \in \boldsymbol{U}_h^1 \times V_h^1$ denote the approximation of $\{\boldsymbol{u}_0^n, p_f^n\}$, $\{\boldsymbol{u}_1^n, p_0^n\}$ and $\{\boldsymbol{u}_*^n, p_*^n\}$ respectively. The backward Euler-Galerkin finite element approximation of Problem M consists in solving:

Problem M$_\mathbf{h}$: For given $\{\boldsymbol{\chi}_h^{\boldsymbol{u}}, \chi_h^p\}$ and $\{\boldsymbol{\chi}_{ijh}^{\boldsymbol{U}}, \boldsymbol{\chi}_{ijh}^P\}$, find, for each time step $n\Delta t$, $n \geq 1$, the pairs $\{\boldsymbol{u}_{0h}^n, p_{fh}^n\} \in \boldsymbol{U}_h^0 \times V_h^0$ and $\{\boldsymbol{u}_{*h}^n, p_{*h}^n\} \in \boldsymbol{U}_h^1 \times V_h^1$ satisfying:

$$
\begin{aligned}
&a_x^*(\boldsymbol{u}_{0h}^n, \boldsymbol{v}_h^0) - (p_{fh}^n, \mathrm{div}_x \boldsymbol{v}_h^0)_0 = F_2^n(\{\widetilde{\boldsymbol{u}_{*h}}^n, \widetilde{p_{*h}}^n\}, \boldsymbol{v}_h^0) + f(\boldsymbol{v}_h^0), \ \forall \boldsymbol{v}_h^0 \in \boldsymbol{U}_h^0 \quad (62) \\
&(\mathrm{div}_x \boldsymbol{u}_{0h}^n, q_h^0)_0 - \Delta t\, d_x(p_{fh}^n, q_h^0) = (\mathrm{div}_x \boldsymbol{u}_{0h}^{n-1}, q_h^0)_0 \quad \forall q_h^0 \in V_h^0
\end{aligned}
$$

and

$$
\begin{aligned}
a_y(\boldsymbol{u}_{*h}^n, \boldsymbol{v}_h^1) - (p_{*h}^n, \mathrm{div}_y \boldsymbol{v}_h^1)_1 = 0 \quad \forall \boldsymbol{v}_h^1 \in \boldsymbol{U}_h^1 \qquad (63) \\
(\mathrm{div}_y \boldsymbol{u}_{*h}^n, q_h^1)_1 + \Delta t\, d_y(p_{*h}^n, q_h^1) = (\mathrm{div}_y \boldsymbol{u}_{1h}^{n-1} + \mathrm{div}_x \boldsymbol{u}_{0h}^{n-1}, q_h^1)_1 \quad \forall q_h^1 \in V_h^1
\end{aligned}
$$

with $(\mathrm{div}_x \boldsymbol{u}_{0h}^0, q_h^0)_0 = (\mathrm{div}_y \boldsymbol{u}_{1h}^0, q_h^1)_1 = 0$.

We remark that the choice of the polynomial degrees of interpolation $\{k^0, l^0\}$ and $\{k^1, l^1\}$ is not totally unconstrained but depends on the stability of Problem

M_h. Numerical analysis of Biot's consolidation problem [14] shows that some combinations of interpolations for displacement and pore pressure (including equal order) lead to unstable finite element approximation with spurious oscillations in the pore pressure field for small t, when the porous medium exhibits nearly incompressible undrained deformations. In particular the initial condition for Problem M_h resembles in form the well known mixed formulation of the incompressible elasticity (or Stokes flow) problem. (see [14]). It is well known that the stability of mixed finite element formulations for the Stokes problem depends on the *inf-sup* (or LBB) condition, see e.g. [14]). On the other hand, it is showed in [12] that these spurious oscillations in the pore pressure field tend to dissipate fastly in time (with order $O(1/t^n)$), where n is related to the degree of interpolation.

5. Numerical Experiments

The performance of the micromechanical computational model is illustrated in a classical example related to the surface subsidence of a naturally fractured oil-field. Fig 2 depicts the idealized macroscopic reservoir geometry. The example was selected as a standard test case though more complex reservoir geometries can also be treated within the same micromechanical formulation.

The periodic microstructure of the fractured reservoir is composed of disjoint rectangular matrix blocks, with side l, surrounded by the interconnected fissure system. The reservoir has height H (selected as H =5L, with L denoting a characteristic macroscopic length) and is subjected to a uniform load of intensity p_e (due to the weight of the overlaying formations) which is applied to the impermeable top interface with a shale formation. The bottom of the reservoir is impermeable and rigid. The representation of the far field solution at a infinite horizontal distance from the well is pursued by introducing an artificial impermeable boundary which also constrains the horizontal component of the displacement. For simplicity consider the case where the macroscopic medium is isotropic with respect to the flow in the macropores, such that $\boldsymbol{K}_F = K_F \boldsymbol{I}$,

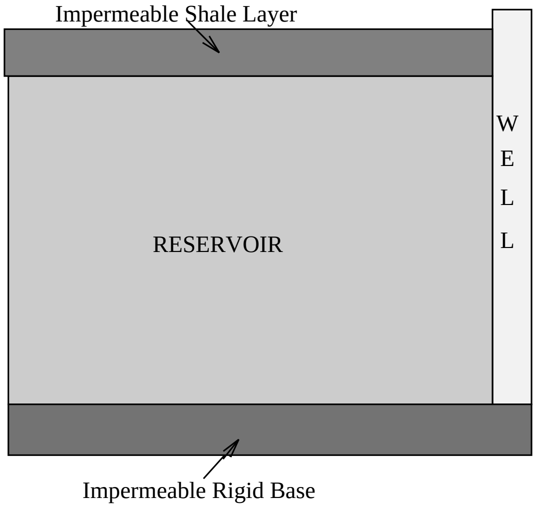

Fig. 2: Case studied related to reservoir compaction

and that the effect of the Poisson coefficient of the reservoir matrix is negligible so that $\lambda_s = \lambda_S = 0$.

We present macroscopic numerical simulations of the problem sketched in Fig. 2 by selecting $n_l = 0.5$, $K_l/K_F = 0.1$ and $l = 0.2L$. In the discretization, we adopt a global mesh of equal order bilinear elements for the macroscopic problem whereas, for each one of the global nodes we associate a local rectangular cell, which is also discretized by equal order bilinear elements. Fig. 3 presents the dimensionless macroscopic vertical displacement of the surface $\boldsymbol{U}^* \equiv 2\boldsymbol{u}_0^n \mu_s/(p_e L)$ as a function of the horizontal distance to the well $X^* = x/L$, for a fixed dimensionless time $T \equiv \mu_s K_F t/L^2 = 150$. The continuous line plot corresponds to the solution which incorporates creep effects related to the delayed cell drainage whereas the dashed line plot was obtained with absence of creep effects, i.e. for an undrained cell response. As one may clearly observe, the numerical results show a strong influence of secondary creep effects on the magnitude of the surface subsidence. It should be noted that the appearance of the small perturbation between the two plots near $X^* = 0$ is due to the introduction of the artificial impermeable boundary representing the far field behavior.

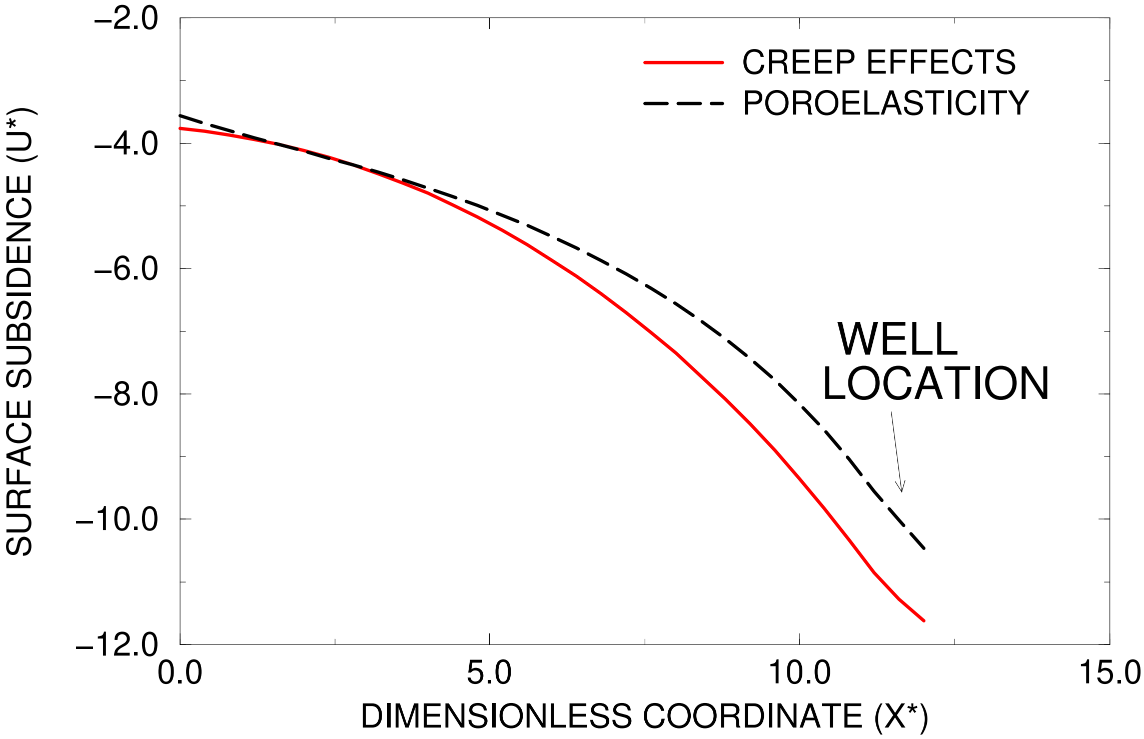

Fig 3: Influence of creep effects on surface subsidence

6. Conclusions

We proposed a new micromechanical computational model for the surface subsidence of a naturally fractured reservoir with a weak formation. The theory was rigorously derived from the asymptotic homogenization technique in conjunction with a two level finite element procedure. The resultant macroscopic model may be embedded in a framework common to numerous microstructure double-porosity models for fractured media. A particular feature of this microstructural model is the ability of providing an accurate portrait of the complex distributed hydro-mechanical interaction between the two systems of matrix blocks and macropores. The understanding of the mechanisms underlying this distributed interaction led to important correlations between reservoir microstructure and macroscopic response, such as secondary creep phenomena which has been classically governed by macroscopic hereditary poroviscoelastic models. Variational principles and two-level finite element approximations were proposed to discretize the governing equations of dual porosity type. The influence of secondary consolidation and creep viscous behavior was illustrated numerically by applying two-scale computations to a problem related to the surface subsidence of a oil-field with disconnected matrix blocks (assumed self-sustained).

Finally the convergence analysis of the homogenization procedure proposed herein can be studied within the framework of the two-scale convergence technique introduced by Allaire [1]. This topic will be a subject of future work.

References

[**1**] Allaire, G., *Homogenization and two-scale convergence*, SIAM J. Math. Analysis, 23(6), (1992), 1482-1518.

[**2**] Arbogast, T., *A simplified dual-porosity model for two-phase flow*, in T.F. Russel et al., Computational Methods in Water Resources, Computational Mechanics Publication, (1992), 419-426.

[**3**] Arbogast, T., *Analysis of the simulation of single phase flow through a naturally fractured reservoir*, SIAM J. Numer. Anal., 26, (1989), 12-29.

[**4**] Beavers, G. S.; Joseph, D. D., *Boundary conditions at a naturally permeable wall*, J. Fluid Mech., 30(1), (1967), 197-207.

[**5**] O. Coussy, *Mechanics of Porous Continua*, John Wiley (1995).

[**6**] Biot, M., *Theory of elasticity and consolidation for a porous anisotropic solid*, J. Appl. Phys., 26, (1955), 182-185.

[**7**] Douglas, J.; Arbogast, T., *Dual porosity models for flow in naturally fractured reservoirs*, in J. H. Cushman, Dynamics of fluid in hierarchical porous media, Academic Press, (1990), 177-222.

[8] Douglas, J.; Peszynska, M.; Showalter, R. E., *Single phase flow in partially fissured media*, Transport in Porous Media, 28(3), (1997), 285-306.

[9] Gripenberg, G.; Londen, S. O.; Staffans, O., *Volterra Integral and Functional Analysis*, Cambridge University Press (1990).

[10] Hornung, U.; Showalter", R. E., *Diffusion models for fractured media, J. Math. Anal. Appl.*",147, (1990), 69-80.

[11] Lewis, R. W.; Sukirman, Y., *Finite element modeling for simulating the surface subsidence above a compacting hydrocarbon reservoir.* Int. J. Num. Anal. Methods Geomech. 18, (1993), 619-639.

[12] Murad, M. A.; Thomée, V.; Loula, A. F. D., *Asymptotic behavior of semidiscrete finite element approximations of Biot's Consolidation Problem*, SIAM J. Num. Anal., 33(3), (1996), 1065-1083.

[13] Murad, M. A.; Cushman, J. H., *Thermomechanical Theories for Swelling Porous Media with Microstructure*, International Journal of Enginnering Science, 38(5), (2000), 517-564.

[14] Murad, M. A.; Loula, A. F. D., *On stability and convergence of finite element approximations of Biot's consolidation problem*, Int. J. Num. Meth. Engrg, 37, (1994), 645-667.

[15] Peszenska, M., *Analysis of an integro-differential equation arising from modeling of flows with fading memory through fissured media*, J. Partial Diff. Eq., 8, (1995), 159-173.

[16] Peszenska, M., *On a model of nonisothermal flow through fissured media*, Diff. and Integral Eqs., 8(6), (1995), 1497-1516.

[17] Ruddy, I.; Anderson, M.; Pattillo, R.; Bishlawi, M.; Foged, N., *Rock compressibility, compaction, and subsidence in a high-porosity chalk reservoir: A case study of Valhall field*, J. of Petroleum Technology, 41(7)), (1989), 741-746.

[18] Saffman, P. G., *On the boundary conditions at the surface of a porous medium*, Studies in applied mathematics, 1(2), (1971), 93-101.

[19] Sanchez-Palencia, E., *Non-homogeneous media and vibration theory*, Lecture Notes in Physics, 127, J. Ehlers (editor), Springer-Verlag (1980)

[20] Simoni, L.; Salomoni, V.; Schreffer", B., *Elastoplastic subsidence models with and without capillary effects*, Comput. Meth. Appl. Mech. Engrg. 171, (1999), 491-502.

[21] Sridharan, A.; Rao, G. V., *Mechanisms controlling the secondary compression of clays*, Geotechnique, 32(3), (1982), 249-260.

Laboratório Nacional de Computação Cientifica (LNCC/MCT)
Av. Getulio Vargas 333
Petrópolis, RJ
e-mail: murad@@lncc.br, joao@@lncc.br, aloc@@lncc.br